Steel and Composite Structures, *Vol. 22, No. 3 (2016) 567-587*
DOI: http://dx.doi.org/10.12989/scs.2016.22.3.567

Plane waves in an anisotropic thermoelastic

Parveen Lata [*1], Rajneesh Kumar [2] and Nidhi Sharma [3]

[1] *Department of Basic and Applied Sciences, Punjabi University, Patiala, Punjab, India*
[2] *Department of Mathematics, Kurukshetra University, Kurukshetra, Haryana, India*
[3] *Department of Mathematics, MM University, Mullana, Ambala, Haryana, India*

(*Received March 19, 2016, Revised October 15, 2016, Accepted October 18, 2016*)

Abstract. The present investigation is to study the plane wave propagation and reflection of plane waves in a homogeneous transversely isotropic magnetothermoelastic medium with two temperature and rotation in the context of GN Type-II and Type-III (1993) theory of thermoelasticity. It is found that, for two dimensional assumed model, there exist three types of coupled longitudinal waves, namely quasi- longitudinal wave (QL), quasi- transverse wave (QTS) and quasi -thermal waves (QT). The different characteristics of waves like phase velocity, attenuation coefficients, specific loss and penetration depth are computed numerically and depicted graphically. The phenomenon of reflection coefficients due to quasi-waves at a plane stress free with thermally insulated boundary is investigated. The ratios of the linear algebraic equations. These amplitude ratios are used further to calculate the shares of different scattered waves in the energy of incident wave. The modulus of the amplitude and energy ratios with the angle of incidence are computed for a particular numerical model. The conservation of energy at the free surface is verified. The effect of energy dissipation and two temperatures on the energy ratios are depicted graphically and discussed. Some special cases of interest are also discussed.

Keywords: phase velocity; attenuation coefficients; specific loss; penetration depth; reflection; energy ratios

1. Introduction

The problem of elastic wave propagation in different media is an important phenomenon in the field of seismology, earthquake engineering and geophysics. The elastic wave propagating through the earth (seismic waves) have to travel through different layers and interfaces. These waves have different velocities and are influenced by the properties of the layer through which they travel. The signals of these waves are not only helpful in providing information about the internal structures of the earth but also helpful in exploration of valuable materials such as minerals, crystals and metals etc. This technique is one of the most suitable in terms of time saving and economy.

As the importance of anisotropic devices has increased in many fields of optics and microwaves, wave propagation in anisotropic media has been widely studied over in the last decades. The anisotropic nature basically stems from the polarization or magnetization that can occur in materials when external fields pass by. Mathematical modeling of plane wave propagation along with the free boundary of an elastic half-space has been subject of continued interest for many years. Keith and Crampin (1977) derived a formulation for calculating the energy division

*Corresponding author, Professor, E-mail: parveenlata@pbi.ac.in

 ISSN: 1229-9367 (Print), 1598-6233 (Online)

among waves generated by plane waves incident on a boundary of anisotropic media. Wave propagation in a microstretch thermoelastic diffusion solid has been investigated by Kumar (2015). Reflection of plane waves at the free surface of a transversely isotropic thermoelastic diffusive solid half-space has been discussed by Kumar and Kansal (2011). Wave propagation has remained the study of concern of many researchers (Kumar and Mukhopadhyay 2010, Lee and Lee 2010, Kumar and Gupta 2013, Othman 2010, Kaushal *et al*. 2011, Kumar *et al*. 2008).

Chen and Gurtin (1968) and Chen *et al*. (1968, 1969) have formulated a theory of heat conduction in deformable bodies which depends upon two distinct temperatures, the conductive temperature φ and the thermo dynamical temperature T. For time independent situations, the difference between these two temperatures is proportional to the heat supply, and in absence of heat supply, the two temperatures are identical. For time dependent problems, the two temperatures are different, regardless of the presence of heat supply. The two temperatures T, φ and the strain are found to have representations in the form of a travelling wave plus a response, which occurs instantaneously throughout the body (Boley and Tolins 1962). The wave propagation in two temperature theory of thermoelasticity was investigated by Warren and Chen (1973).

Green and Naghdi (1991) postulated a new concept in thermoelasticity theories and proposed three models which are subsequently referred to as GN-I, II, and III models. The linearised version of model-I corresponds to classical thermoelastic model (based on Fourier's law). The linearised version of model-II and III permit propagation of thermal waves at finite speed. Green-Naghdi's second model (GN-II), in particular exhibits a feature that is not present in other established thermoelastic models as it does not sustain dissipation of thermal energy (Green and Naghdi 1993). In this model, the constitutive equations are derived by starting with the reduced energy equation and by including the thermal displacement gradient among other constitutive variables. Green-Naghdi's third model (GN-III) admits dissipation of energy. In this model the constitutive equations are derived by starting with the reduced energy equation, where the thermal displacement gradient in addition to the temperature gradient, are among the constitutive variables. Green and Naghdi (1992) included the derivation of a complete set of governing equations of a linearised version of the theory for homogeneous and isotropic materials in terms of the displacement and temperature fields and a proof of the uniqueness of the solution for the corresponding initial boundary value problem.

A comprehensive work has been done in thermoelasticity theory with and without energy dissipation and thermoelasticity with two temperature. Youssef (2011) constructed a new theory of generalized thermoelasticity by taking into account two-temperature generalized thermoelasticity theory for a homogeneous and isotropic body without energy dissipation. Several researchers studied various problems involving two temperature (e.g., Youssef 2006, Sharma and Marin 2013, Sharma and Bhargav 2014, Sharma *et al*. 2013, Sharma and Kumar 2013).

In view of the fact that most of the large bodies like the earth, the moon and other planets have an angular velocity, as well as earth itself behaves like a huge magnet, it is important to study the propagation of thermoelastic waves in a rotating medium under the influence of magnetic field. So, the attempts are being made to study the propagation of finite thermoelastic waves in an infinite elastic medium rotating with angular velocity. Several authors (Das and Kanoria 2014, Atwa and Jahangir 2014, Marin 1995, 2010, Marin and Marinescu 1998) have studied various problems in generalized thermoelasticity to study the effect of rotation.

Here in this paper, we analyse the reflection of plane waves incident at the stress free, thermally insulated surface of a homogeneous, transversely isotropic magnetothermoelastic solid with two temperature along with rotation in the context of GN Type-II and Type-III theory of thermo-

elasticity. The graphical representation is given for amplitude and energy ratios of various reflected waves to that of incident waves for different values of incident angle. Also phase velocity and attenuation coefficients of plane waves are computed and presented graphically for different values of wave frequency.

2. Basic equations

Following Zakaria (2014), the simplified Maxwell's linear equation of electrodynamics for a slowly moving and perfectly conducting elastic solid are

$$\text{curl}\,\vec{h} = \vec{J} + \varepsilon_0 \frac{\partial \vec{E}}{\partial t} \tag{1}$$

$$\text{curl}\vec{E} = -\mu_0 \frac{\partial \vec{h}}{\partial t} \tag{2}$$

$$\vec{E} = -\mu_0 \left(\frac{\partial \vec{u}}{\partial t} \times \overrightarrow{H_0}\right) \tag{3}$$

$$\text{div}\vec{h} = 0 \tag{4}$$

Maxwell stress components are given by

$$T_{ij} = \mu_0 (H_i h_j + H_j h_i - H_k h_k \delta_{ij}) \tag{5}$$

where $\overrightarrow{H_0}-$ the external applied magnetic field intensity vector, $\vec{h}-$ the induced magnetic field vector, $\vec{E}-$ the induced electric field vector, $\vec{J}-$ the current density vector, $\vec{u}-$ is the displacement vector, μ_0 and ε_0- the magnetic and electric permeabilities respectively, $T_{ij}-$ the component of Maxwell stress tensor and $\delta_{ij}-$ the Kronecker delta.

The constitutive relations for a transversely isotropic thermoelastic medium are given by

$$t_{ij} = C_{ijkl}\, e_{kl} - \beta_{ij}\, T \tag{6}$$

Equation of motion for a transversely isotropic thermoelastic medium rotating uniformly with an angular velocity $\boldsymbol{\Omega} = \Omega n$, where *n* is a unit vector representing the direction of axis of rotation and taking into account Lorentz force

$$t_{ij,j} + F_i = \rho\{\ddot{u}_i + \left(\boldsymbol{\Omega} \times (\boldsymbol{\Omega} \times u)\right)_i + (2\boldsymbol{\Omega} \times \dot{u})_i \tag{7}$$

The heat conduction equation following Chandrasekharaiah (1998) and Youssef (2011) is

$$K_{ij}\, \varphi_{,ij} + K_{IJ}^{*}\, \dot{\varphi}_{ij} = \beta_{ij}\, T_0 \ddot{e_{ij}} + \rho C_E \ddot{T} \tag{8}$$

The strain displacement relations are

$$e_{ij} = \frac{1}{2}\left(u_{i,j} + u_{j,i}\right) \qquad i,j = 1,2,3$$

where $F_i = \mu_0(\vec{J} \times \overrightarrow{H_0})_i$ are the components of Lorentz force.

$$\beta_{ij} = C_{ijkl}\,\alpha_{ij} \qquad \text{and} \qquad T = \varphi - a_{ij}\,\varphi_{,ij}$$

$$\beta_{ij} = \beta_i \delta_{ij}\,, \quad K_{ij} = K_i \delta_{ij}\,, \quad K_{ij}{}^{*} = K_i{}^{*} \delta_{ij}\,, \qquad i \quad \text{is not summed}$$

$C_{ijkl}\,(C_{ijkl} = C_{klij} = C_{jikl} = C_{ijlk})$ are elastic parameters, β_{ij} is the thermal tensor, T is the temperature, T_0 is the reference temperature, t_{ij} are the components of stress tensor, e_{kl} are the components of strain tensor, u_i are the displacement components, ρ is the density, C_E is the specific heat, K_{ij} is the materialistic constant, K_{IJ}^{*} is the thermal conductivity, a_{ij} are the two temperature parameters, α_{ij} is the coefficient of linear thermal expansion, Ω is the angular velocity of the solid.

3. Formulation and solution of the problem

We consider a homogeneous perfectly conducting transversely isotropic magnetothermoelastic medium with two temperature and rotation in the context of GN Type-II and Type-III theory of thermoelasticity initially at a uniform temperature T_0. The origin of rectangular Cartesian co-ordinate system (x_1, x_2, x_3) is taken at any point on the plane horizontal surface. We take $x_3 -$ axis along the axis material symmetry and pointing vertically downwards into the medium, which is thus represented by $x_3 \geq 0$. The surface ($x_3 = 0$) is subjected to stress free, thermally insulated boundary conditions. We choose $x_1 -$ axis in the direction of wave propagation so that all particles on a line parallel to $x_2 -$ axis are equally displaced. Therefore, all the field quantities will be independent of $x_2 -$ co-ordinate. Following Slaughter (2002), using appropriate transformations, on the set of Eqs. (6)-(7), we derive the basic equations for transversely isotropic thermoelastic solid. The components of displacement vector $\vec{u}$ and conductive temperature φ for the two dimensional problem have the form

$$\vec{u}(x_1, x_3, t) = (u_1, 0, u_3), \qquad \text{and} \qquad \varphi = \varphi(x_1, x_3, t) \tag{9}$$

We also assume that

$$\mathbf{\Omega} = (0, \Omega, 0) \tag{10}$$

From the generalized Ohm's law

$$J_2 = 0 \tag{11}$$

the current density components J_1 and J_3 are given as

$$J_1 = -\varepsilon_0 \mu_0 H_0 \frac{\partial^2 u_3}{\partial t^2} \tag{12}$$

$$J_3 = \varepsilon_0 \mu_0 H_0 \frac{\partial^2 u_1}{\partial t^2} \tag{13}$$

Eqs. (7) and (8) with the aid of Eqs. (9)-(13), yield

$$c_{11}\frac{\partial^2 u_1}{\partial {x_1}^2}+c_{13}\frac{\partial^2 u_3}{\partial x_1 \partial x_3}+c_{44}\left(\frac{\partial^2 u_1}{\partial {x_3}^2}+\frac{\partial^2 u_3}{\partial x_1 \partial x_3}\right)$$
$$-\beta_1\frac{\partial}{\partial x_1}\left\{\varphi-\left(a_1\frac{\partial^2 \varphi}{\partial {x_1}^2}+a_3\frac{\partial^2 \varphi}{\partial {x_3}^2}\right)\right\}-\mu_0 J_3 H_0=\rho\left(\frac{\partial^2 u_1}{\partial t^2}-\Omega^2 u_1+2\Omega\frac{\partial u_3}{\partial t}\right) \tag{14}$$

$$(c_{13}+c_{44})\frac{\partial^2 u_1}{\partial x_1 \partial x_3}+c_{44}\frac{\partial^2 u_3}{\partial {x_1}^2}+c_{33}\frac{\partial^2 u_3}{\partial {x_3}^2}-\beta_3\frac{\partial}{\partial x_3}\left\{\varphi-\left(a_1\frac{\partial^2 \varphi}{\partial {x_1}^2}+a_3\frac{\partial^2 \varphi}{\partial {x_3}^2}\right)\right\}$$
$$+\mu_0 J_1 H_0=\rho\left(\frac{\partial^2 u_3}{\partial t^2}-\Omega^2 u_3-2\Omega\frac{\partial u_1}{\partial t}\right) \tag{15}$$

$$\left(k_1+{k_1}^*\frac{\partial}{\partial t}\right)\frac{\partial^2 \varphi}{\partial {x_1}^2}+\left(k_3+{k_3}^*\frac{\partial}{\partial t}\right)\frac{\partial^2 \varphi}{\partial {x_3}^2}=T_0\frac{\partial^2}{\partial t^2}\left\{\beta_1\frac{\partial u_1}{\partial x_1}+\beta_3\frac{\partial u_3}{\partial x_3}\right\}+\rho C_E\ddot{T} \tag{16}$$

and

$$t_{11}=c_{11}e_{11}+c_{13}e_{33}-\beta_1 T \tag{17}$$

$$t_{33}=c_{13}e_{11}+c_{33}e_{33}-\beta_3 T \tag{18}$$

$$t_{13}=2c_{44}e_{13} \tag{19}$$

where $T=\varphi-\left(a_1\frac{\partial^2\varphi}{\partial x_1^2}+a_3\frac{\partial^2\varphi}{\partial x_3^2}\right)$, $\beta_1=(c_{11}+c_{12})\alpha_1+c_{13}\alpha_3$, $\beta_3=2c_{13}\alpha_1+c_{33}\alpha_3$.

In the above equations we use the contracting subscript notations $(11\rightarrow 1, 22\rightarrow 2, 33\rightarrow 3, 23\rightarrow 4, 31\rightarrow 5, 12\rightarrow 6)$ to relate c_{ijkl} *to* c_{mn}.

To facilitate the solution, following dimensionless quantities are introduced

$$x_1'=\frac{x_1}{L},\ x_3'=\frac{x_3}{L},\ u_1'=\frac{\rho c_1^2}{L\beta_1 T_0}u_1,\ u_3'=\frac{\rho c_1^2}{L\beta_1 T_0}u_3,\ T'=\frac{T}{T_0},\ t'=\frac{c_1}{L}t,\ t_{11}'=\frac{t_{11}}{\beta_1 T_0},$$
$$t_{33}'=\frac{t_{33}}{\beta_1 T_0},\ t_{31}'=\frac{t_{31}}{\beta_1 T_0},\ \varphi'=\frac{\varphi}{T_0},\ a_1'=\frac{a_1}{L},\ a_3'=\frac{a_3}{L},\ h'=\frac{h}{H_0},\ \Omega'=\frac{L}{C_1}\Omega \tag{20}$$

Making use of Eq. (20) in Eqs. (14)-(16), after suppressing the primes, yield

$$\frac{\partial^2 u_1}{\partial {x_1}^2}+\delta_4\frac{\partial^2 u_3}{\partial x_1 \partial x_3}+\delta_2\left(\frac{\partial^2 u_1}{\partial {x_3}^2}+\frac{\partial^2 u_3}{\partial x_1 \partial x_3}\right)-\frac{\partial}{\partial x_1}\left\{\varphi-\left(\frac{a_1}{L}\frac{\partial^2 \varphi}{\partial {x_1}^2}+\frac{a_3}{L}\frac{\partial^2 \varphi}{\partial {x_3}^2}\right)\right\}$$
$$=\left(\frac{\varepsilon_0\mu_0^2 H_0^2}{\rho}+1\right)\frac{\partial^2 u_1}{\partial t^2}-\Omega^2 u_1+2\Omega\frac{\partial u_3}{\partial t} \tag{21}$$

$$\delta_1 \frac{\partial^2 u_1}{\partial x_1 \partial x_3} + \delta_2 \frac{\partial^2 u_3}{\partial {x_1}^2} + \delta_3 \frac{\partial^2 u_3}{\partial {x_3}^2} - \frac{\beta_3}{\beta_1} \frac{\partial}{\partial x_3} \left\{ \varphi - \left(\frac{a_1}{L} \frac{\partial^2 \varphi}{\partial {x_1}^2} + \frac{a_3}{L} \frac{\partial^2 \varphi}{\partial {x_3}^2} \right) \right\}$$
$$= \left(\frac{\varepsilon_0 \mu_0^2 H_0^2}{\rho} + 1 \right) \frac{\partial^2 u_3}{\partial t^2} - \Omega^2 u_3 - 2\Omega \frac{\partial u_1}{\partial t} \tag{22}$$

$$\varepsilon_1 \left(1 + \frac{\varepsilon_3}{\varepsilon_1} \frac{\partial}{\partial t} \right) \frac{\partial^2 \varphi}{\partial {x_1}^2} + \varepsilon_2 \left(1 + \frac{\varepsilon_4}{\varepsilon_2} \frac{\partial}{\partial t} \right) \frac{\partial^2 \varphi}{\partial {x_3}^2}$$
$$= \varepsilon_5{}' {\beta_1}^2 \frac{\partial^2}{\partial t^2} \left(\frac{\partial u}{\partial x_1} + \frac{\beta_3}{\beta_1} \frac{\partial u_3}{\partial x_3} \right) + \frac{\partial^2}{\partial t^2} \left(\left\{ \varphi - \frac{a_1}{L} \frac{\partial^2 \varphi}{\partial {x_1}^2} + \frac{a_3}{L} \frac{\partial^2 \varphi}{\partial {x_3}^2} \right\} \right) \tag{23}$$

$$\delta_1 = \frac{(c_{13} + c_{44})}{c_{11}}, \quad \delta_2 = \frac{c_{44}}{c_{11}}, \quad \delta_3 = \frac{c_{33}}{c_{11}}, \quad \delta_4 = \frac{c_{13}}{c_{11}},$$
$$\varepsilon_1 = \frac{k_1}{\rho C_E c_1^2}, \quad \varepsilon_2 = \frac{k_3}{\rho C_E c_1^2}, \quad \varepsilon_3 = \frac{{k_1}^*}{L \rho C_E c_1}, \quad \varepsilon_4 = \frac{{k_3}^*}{L \rho C_E c_1}, \quad \varepsilon_5{}' = \frac{T_0}{\rho^2 C_E c_1^2}$$

4. Plane wave propagation

We seek plane wave solution of the equations of the form

$$\begin{pmatrix} u_1 \\ u_3 \\ \varphi \end{pmatrix} = \begin{pmatrix} U_1 \\ U_3 \\ \varphi^* \end{pmatrix} \exp\{i(\omega t - \xi(x_1 \sin\theta - x_3 \cos\theta))\} \tag{24}$$

where $(\sin\theta, \cos\theta)$ denotes the projection of the wave normal onto the $x_1 - x_3$ plane, ξ and ω are respectively the wave number and angular frequency of plane waves propagating in $x_1 - x_3$ plane.

Upon using Eq. (24) in Eqs. (21)-(23) and then eliminating U_1, U_3 and φ^* from the resulting equations yields the following characteristic equation

$$A\xi^6 + B\xi^4 + C\xi^2 + D = 0 \tag{25}$$

Where $A = \zeta_4 \zeta_5 \zeta_6 - cos^2\theta\, \zeta_2 \zeta_7 p_1 - \delta_1 \zeta_8^2 \zeta_1 \zeta_4 + \zeta_2 \zeta_7 \zeta_8 + \zeta_2 \zeta_7 \zeta_8^2 \zeta_1$

$$B = -\zeta_1 \zeta_4 \zeta_6 - \zeta_1 cos^2\theta\, \zeta_2 \zeta_7 p_1 + \omega^2 \zeta_6 \zeta_5 - \zeta_4 \zeta_5 \zeta_1 + \zeta_5 cos^2\theta\, \zeta_7 p_1 - \delta_1 \zeta_4 \zeta_3 \zeta_8$$
$$+\zeta_2 \zeta_7 \zeta_8 - \delta_1 \omega^2 \zeta_1 \zeta_8^2 + \zeta_3 \zeta_8 \zeta_1 \zeta_4 - \zeta 1_8^2 \zeta_1 \zeta_7 - \zeta_2 \zeta_8 \zeta_3 \zeta_7 + \delta_1 \zeta_8 \zeta_7$$
$$+p_1 \zeta_7 \zeta_6 sin^2\theta - sin^2\theta\, \zeta_2 \zeta_7 p_1$$

$$C = -\zeta_5 \zeta_1 \omega^2 - \zeta_1 \zeta_6 \omega^2 + \zeta_1^2 \zeta_4 - \zeta_1 cos^2\theta\, \zeta_7 p_1 - \zeta_3 \delta_1 \omega^2 \zeta_8 + \zeta_3^2 \zeta_4$$
$$+\zeta_8 \zeta_3 \zeta_1 \omega^2 - \zeta_1\, \varepsilon_5{}' \beta_1^2 \omega^2 sin^2\theta$$

$$D = \omega^2(\zeta_1^2 - \zeta_3^2)$$

$$\zeta_1 = \left(\frac{\varepsilon_0 \mu_0^2 H_0^2}{\rho} + 1\right)\omega^2 + \Omega^2, \qquad \zeta_2 = \frac{a_1}{L} sin^2\theta + \frac{a_3}{L} cos^2\theta, \;\; \zeta_3 = 2i\omega\Omega,$$

$$\zeta_4 = \zeta_2\omega^2 - sin^2\theta(\varepsilon_1 + i\varepsilon_3) - cos^2\theta\,(\varepsilon_2 + i\varepsilon_4), \quad \zeta_5 = sin^2\theta + \delta_2 cos^2\theta,$$

$$\zeta_6 = \delta_2 sin^2\theta + \delta_3 cos^2\theta, \quad \zeta_7 = \varepsilon_5{}'\omega^2\beta_1\beta_3, \quad \zeta_8 = sin\theta cos\theta, \quad p_5 = \frac{\beta_3}{\beta_1}$$

The roots of Eq. (25) gives six values of ξ, in which we are interested to those roots whose imaginary parts are positive. Corresponding to these roots, there exists three waves corresponding to decreasing orders of their velocities, namely quasi-longitudinal, quasi-transverse and quasi-thermal waves. The phase velocities, attenuation coefficients, specific loss and penetration depth of these waves are obtained by the following expressions.

(*i*) *Phase velocity*

The phase velocity is given by

$$V_j = \frac{\omega}{\left|Re(\xi_j)\right|}, \qquad j = 1, 2, 3$$

where V_j, j=1,2,3 are the phase velocities of QL, QTS and QT waves respectively.

(*ii*) *Attenuation coefficient*

The attenuation coefficient is defined by

$$Q_j = Im(\xi_j), \qquad j = 1, 2, 3$$

where $Q_j, j = 1, 2, 3$ are the attenuation coefficients of QL, QTS and QT waves respectively.

(*iii*) *Specific loss*

The specific loss is the ratio of energy (Δw) dissipated in taking a specimen through a stress cycle, to the elastic energy (w) stored in the specimen when the strain is maximum. The specific loss is the most direct method of defining internal fraction of a material. For a sinusoidal plane wave of small amplitude, the specific loss $\left(\frac{\Delta w}{w}\right)$ equals 4π times the absolute value of the imaginary part of ξ to the real part of ξ, i.e.

$$R_i = \left(\frac{\Delta w}{w}\right)_j = 4\pi \left|\frac{Im(\xi_j)}{Re(\xi_{j)}}\right|, \qquad j = 1, 2, 3$$

where R_1, R_2, R_3 are the specific losses of QL, QTS and QT waves respectively.

(*iv*) *Penetration depth*

The penetration depth is defined $S_j = \frac{1}{\left|Im(\xi_j)\right|}, j = 1, 2, 3$ by

where S_1 is the penetration depth of QL (quasi longitudinal) wave, S_2 is the penetration depth of QTS (quasi transverse) wave, S_3 is the penetration depth of QT (quasi thermal) wave.

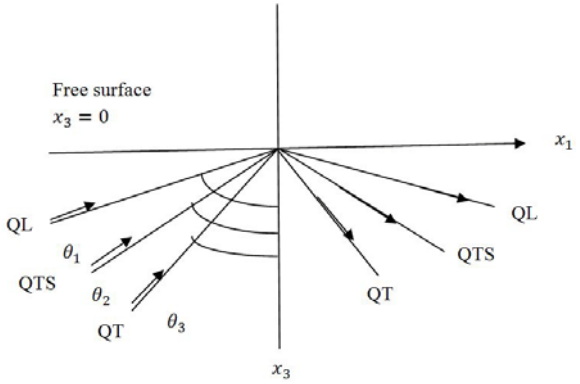

Fig. 1 Geometry of the problem

5. Reflection and transmission at the boundary surfaces

We consider a homogeneous transversely isotropic magnetothermoelastic half-space occupying the region $x_3 \geq 0$. Incident quasi-longitudinal or quasi-transverse or quasithermal waves at the stress free, thermally insulated surface ($x_3 = 0$) will generate reflected QL, reflected QTS and reflected QT waves in the half-space $x_3 > 0$. The total displacements, conductive temperature are given by

$$u_1 = \sum_{j=1}^{6} A_j e^{iM_j}, \quad u_3 = \sum_{j=1}^{6} d_j A_j e^{iM_j}, \quad \varphi = \sum_{j=1}^{6} l_j A_j e^{iM_j}, \quad j = 1, 2\ldots, 6 \tag{26}$$

where

$$M_j = \omega t - \xi_j \left(x_1 sin\theta_j - x_3 cos\theta_j\right), \qquad j = 1, 2, 3$$

$$M_j = \omega t - \xi_j \left(x_1 sin\theta_j + x_3 cos\theta_j\right), \qquad j = 4, 5, 6$$

Here subscripts j = 1, 2, 3 respectively denote the quantities corresponding to incident QL, QTS and QT-mode, whereas the subscripts j=4,5,6 denote the corresponding reflected waves, ξ_j are the roots obtained from Eq. (25).

$$d_j = \frac{\xi_j^4\left(\zeta_{8j}\zeta_{2j}\zeta_{7j} - \delta_1\zeta_{8j}\zeta_{4j}\right) + \xi_j^2\zeta_{8j}\left(\zeta_{7j} - \delta_1\omega^2\right) + \zeta_{3j}\omega^2(1 + \zeta_{4j})}{-\xi_j^4\left(\zeta_{6j}\zeta_{4j} + \zeta_{7j}\zeta_{2j}cos\theta_j{}^2\, p_1\right) + \xi_j^2(\zeta_{4j}\zeta_{1j} - \zeta_{7j}cos\theta_j{}^2\, p_1 - \omega^2\zeta_{6j})}, \quad j = 1, 2, 3$$

$$l_j = \frac{-i\xi_j^3\zeta_{7j}\left(\zeta_{8j}cos\theta_j\,\delta_1 - p_1\zeta_{6j}sin\theta_j\right) + i\xi_j\zeta_{7j}\left(\zeta_{3j}cos\theta_j + p_1 sin\theta_j\zeta_{1j}\right)}{-\xi_j^4\left(\zeta_{6j}\zeta_{4j} + \zeta_{7j}\zeta_{2j}cos\theta_j{}^2\, p_1\right) + \xi_j^2(\zeta_{4j}\zeta_{1j} - \zeta_{7j}cos\theta_j{}^2\, p_1 - \omega^2\zeta_{6j})}, \quad j = 1, 2, 3$$

$$d_j = \frac{\xi_j^4\left(-\zeta_{8j}\zeta_{2j}\zeta_{7j} + \delta_1\zeta_{8j}\zeta_{4j}\right) - \xi_j^2\zeta_{8j}\left(\zeta_{7j} - \delta_1\omega^2\right) + \zeta_{3j}\omega^2(1 + \zeta_{4j})}{-\xi_j^4\left(\zeta_{6j}\zeta_{4j} + \zeta_{7j}\zeta_{2j}cos\theta_j{}^2\, p_1\right) + \xi_j^2(\zeta_{4j}\zeta_{1j} - \zeta_{7j}cos\theta_j{}^2\, p_1 - \omega^2\zeta_{6j})}, \quad j = 4, 5, 6$$

$$l_j = \frac{-i\xi_j^3\zeta_{7j}\left(-\zeta_{8j}cos\theta_j\,\delta_1 - p_1\zeta_{6j}sin\theta_j\right) + i\xi_j\zeta_{7j}\left(-\zeta_{3j}cos\theta_j + p_1 sin\theta_j\,\zeta_{1j}\right)}{-\xi_j^4\left(\zeta_{6j}\zeta_{4j} + \zeta_{7j}\zeta_{2j}cos\theta_j{}^2\,p_1\right) + \xi_j^2(\zeta_{4j}\zeta_{1j} - \zeta_{7j}cos\theta_j{}^2\,p_1 - \omega^2\zeta_{6j})},\ \ j = 4,5,6$$

6. Boundary conditions

The dimensionless boundary conditions at the free surface $x_3 = 0$, are given by

$$(i)\quad t_{33} = 0 \tag{27}$$

$$(ii)\quad t_{31} = 0 \tag{28}$$

$$(iii)\quad \frac{\partial\varphi}{\partial x_3} = 0 \tag{29}$$

Making use of Eq. (26) into the boundary conditions Eqs. (27)-(29), we obtain

$$\begin{aligned}&\sum_{j=1}^{3}(-i\xi_j sin\theta_j\,\frac{c_{13}}{\rho c_1^2} + id_j\xi_j\,\frac{c_{33}}{\rho c_1^2} - p_1 l_j\,(1 + a_1\xi_j^2 sin\theta_j{}^2 + a_3 cos\theta_j{}^2))\,A_j\,e^{iM_j(x_1,0)}\\ &+\sum_{j=4}^{6}(-i\xi_j sin\theta_j\,\frac{c_{13}}{\rho c_1^2} - id_j\xi_j\,\frac{c_{33}}{\rho c_1^2} - p_1 l_j\,(1 + a_1\xi_j^2 sin\theta_j{}^2 + a_3 cos\theta_j{}^2))\,A_j\,e^{iM_j(x_1,0)} = 0\end{aligned} \tag{30}$$

$$\begin{aligned}&\sum_{j=1}^{3}(-i\xi_j sin\theta_j + id_j\xi_j cos\theta_j)\,A_j\,e^{iM_j(x_1,0)}\\ &+\sum_{j=4}^{6}(-i\xi_j sin\theta_j - id_j\xi_j cos\theta_j)\,A_j\,e^{iM_j(x_1,0)} = 0\end{aligned} \tag{31}$$

$$\sum_{j=1}^{3}(i\xi_j cos\theta_j\,l_j + h_1 l_j)\,A_j\,e^{iM_j(x_1,0)} + \sum_{j=4}^{6}(-i\xi_j cos\theta_j\,l_j + h_1 l_j)\,A_j\,e^{iM_j(x_1,0)} = 0 \tag{32}$$

The Eqs. (30)-(32) are satisfied for all values of x_1, therefore we have

$$M_1(x_1,0) = M_2(x_1,0) = M_3(x_1,0) = M_4(x_1,0) = M_5(x_1,0) = M_6(x_1,0) \tag{33}$$

From Eqs. (26) and (33), we obtain

$$\xi_1 sin\theta_1 = \xi_2 sin\theta_2 = \xi_3 sin\theta_3 = \xi_4 sin\theta_4 = \xi_5 sin\theta_5 = \xi_6 sin\theta_6 \tag{34}$$

which is the form of Snell's law for stress free, thermally insulated surface of transversely isotropic magnetothermoelastic medium with rotation. Eqs. (30)-(32) and (34) yield

$$\sum_{q=1}^{3} X_{iq}A_q + \sum_{j=4}^{6} X_{ij}A_j = 0, \qquad (i = 1,2,3) \tag{35}$$

where

$$\begin{aligned}
X_{1q} &= -i\xi_q sin\theta_q \frac{c_{13}}{\rho c_1^2} + id_q\xi_q \frac{c_{33}}{\rho c_1^2} - p_1 l_q\left(1 + a_1\xi_q^2 sin\theta_q{}^2 + a_3 cos\theta_q{}^2\right), \qquad q = 1,2,3\\
X_{2q} &= -i\xi_q sin\theta_q + id_q\xi_q cos\theta_q, \qquad q = 1,2,3\\
X_{3q} &= i\xi_q cos\theta_q l_q + h_1 l_q, \qquad q = 1,2,3\\
X_{1j} &= -i\xi_j sin\theta_j \frac{c_{13}}{\rho c_1^2} - id_j\xi_j \frac{c_{33}}{\rho c_1^2} - p_1 l_j\left(1 + a_1\xi_j^2 sin\theta_j{}^2 + a_3 cos\theta_j{}^2\right), \qquad j = 4,5,6\\
X_{2j} &= -i\xi_j sin\theta_j - id_j\xi_j cos\theta_j, \qquad j = 4,5,6\\
X_{3j} &= -i\xi_j cos\theta_j l_j + h_1 l_j, \qquad j = 4,5,6
\end{aligned} \tag{36}$$

Incident QL-wave

In case of quasi-longitudinal wave, the subscript q takes only one value, that is q=1, which means $A_2 = A_3 = 0$. Dividing the set of equations (35) throughout by A_1, we obtain a system of three homogeneous equations in three unknowns which can be solved by Cramer's rule and we have

$$A_{1i} = \frac{A_{i+3}}{A_1} = \frac{\Delta_i^1}{\Delta}, \qquad i = 1,2,3 \tag{37}$$

Incident QTS-wave

In case of quasi-transverse wave, the subscript q takes only one value, that is q=*2*, which means $A_1 = A_3 = 0$. Dividing the set of equations (35) throughout by A_2, we obtain a system of three homogeneous equations in three unknowns which can be solved by Cramer's rule and we have

$$A_{2i} = \frac{A_{i+3}}{A_2} = \frac{\Delta_i^1}{\Delta}, \qquad i = 1,2,3 \tag{38}$$

Incident QT-wave

In case of quasi-thermal wave, the subscript q takes only one value, that is q = 3, which means $A_1 = A_2 = 0$. Dividing the set of Eq. (35) throughout by A_3, we obtain a system of three homogeneous equations in three unknowns which can be solved by Cramer's rule and we have

$$A_{3i} = \frac{A_{i+3}}{A_3} = \frac{\Delta_i^1}{\Delta}, \qquad i = 1,2,3 \tag{39}$$

where Z_i (i = 1, 2, 3) are the amplitude ratios of the reflected QL, reflected QTS, reflected QT - waves to that of the incident QL-(QTS or QT) waves respectively.

Here $\Delta = |A_{ii+3}|_{3\times 3}$ and Δ_i^p (*i=1,2,3*) can be obtained by replacing, respectively, the 1st, 2nd and 3rd columns of Δ by $\left[-X_{1p}, -X_{2p}, -X_{3p}\right]^t$.

Following Achenbach (1973), the energy flux across the surface element, which is the rate at which the energy is communicated per unit area of the surface is represented as

$$P^* = t_{lm} n_m \dot{u}_l \tag{40}$$

where t_{lm} is the stress tensor, n_m are the direction cosines of the unit normal and $\dot{u}_l$ are the components of the particle velocity.

The time average of P^* over a period, denoted by $< P^* >$, represents the average energy transmission per unit surface area per unit time and is given at the interface $x_3 = 0$ as

$$< P^* > =< Re\,(t_{13}).Re\,(\dot{u}_1) + Re(t_{33})Re(\dot{u}_3) > \tag{41}$$

Following Achenbach (1973), for any two complex functions *f* and *g*, we have

$$< Re(f) >< Re(g) > = \frac{1}{2} Re(f\bar{g}). \tag{42}$$

The expressions for energy ratios $E_i, (i = 1,2,3)$ for reflected QL, QT, QTH-wave are given as

(*i*) *In case of incident QL- wave*

$$E_{1i} = \frac{< P^*_{i+3} >}{< P^*_1 >}, \qquad i = 1, 2, 3 \tag{43}$$

(*ii*) *In case of incident QTS- wave*

$$E_{2i} = \frac{< P^*_{i+3} >}{< P^*_2 >}, \qquad i = 1, 2, 3 \tag{44}$$

(*iii*) *In case of incident QT- wave*

$$E_{3i} = \frac{< P^*_{i+3} >}{< P^*_3 >}, \qquad i = 1, 2, 3 \tag{45}$$

Where $< P^*_i >$, i = 1, 2, 3 are the average energies transmission per unit surface area per unit time corresponding to incident QL, QTS, QT waves respectively and $< P^*_{i+3} >$, i = 1, 2, 3 are the average energies transmission per unit surface area per unit time corresponding to reflected QL, QTS, QT waves respectively.

7. Particular cases

(1) If ${k_1}^* = {k_3}^* = 0$, then we obtain the resulting expressions for transversely isotropic thermoelastic solid with rotation and without energy dissipation and with two temperature.

(2) If $\Omega = 0$, then we obtain the resulting expressions for transversely isotropic thermoelastic solid with and without energy dissipation and with two temperature without rotation.

(3) If $a_1 = a_3 = 0$, then we obtain the corresponding expressions for displacements, and stresses and conductive temperature for transversely isotropic thermoelastic solid with rotation and with and without energy dissipation.

(4) If we take $c_{11} = \lambda + 2\mu = c_{33}$, $c_{12} = c_{13} = \lambda$, $c_{44} = \mu$, $\beta_1 = \beta_3 = \beta$, $\alpha_1 = \alpha_3 = \alpha$, $K_1 = K_3 = K, a_1 = a_3 = a$, we obtain the corresponding expressions for displacements, and stresses and conductive temperature for isotropic thermoelastic solid with combined effects of rotation, two temperature and with and without energy dissipation.

8. Numerical results and discussion

For the purpose of numerical calculation, we consider the cases of incident QL,QTS, QT waves respectively and take the stress free thermally insulated boundary conditions. Copper material is chosen for the purpose of numerical calculation (Dhaliwal and Singh 1980) with numerical values as

$$c_{11} = 18.78 \times 10^{10}\ Kgm^{-1}s^{-2},\quad c_{12} = 8.76 \times 10^{10}\ Kgm^{-1}s^{-2},$$
$$c_{13} = 8.0 \times 10^{10}\ Kgm^{-1}s^{-2},\quad c_{33} = 17.2 \times 10^{10}\ Kgm^{-1}s^{-2},$$
$$c_{44} = 5.06 \times 10^{10}\ Kgm^{-1}s^{-2},\quad C_E = 0.6331 \times 10^{3} JKg^{-1}K^{-1},$$
$$\alpha_1 = 2.98 \times 10^{-5}K^{-1},\quad \alpha_3 = 2.4 \times 10^{-5}K^{-1},\quad \rho = 8.954 \times 10^{3} Kgm^{-3},$$
$${K_1}^* = 0.433 \times 10^{3} Wm^{-1}K^{-1},\quad {K_3}^* = 0.450 \times 10^{3} Wm^{-1}K^{-1},$$
$$K_1 = 0.02 \times 10^{2} Nsec^{-2}deg^{-1},\quad K_3 = 0.04 \times 10^{2} Nsec^{-2}deg^{-1}.$$

The values of two temperatures, frequency ω, rotation Ω, magnetic effect H_0, are taken as 0.03,0.06, $10S^{-1}$, 4.0,1.2 respectively.

The software Matlab 8.0.4 has been used to determine the values of phase velocity, attenuation coefficient, specific loss, penetration depth, energy ratios and amplitude ratios of reflected QL, QTS and QT waves with respect to incident QL, QTS, and QT waves respectively. The variations of phase velocity, attenuation coefficients, specific loss and penetration depth with respect to frequency are shown in Figs. 2-13. The variation of magnitude of energy ratios of reflected waves subject to incident waves have been plotted in the Figs. 14-22 with respect to angle of incidence. The variation of magnitude of amplitude ratios have been plotted in the Figs. 23-31 with respect to angle of incidence.

A comparison has been made to show the effect of energy dissipation and two temperature on the various quantities.

(1) Solid line corresponds to the case of with and without energy dissipation (GN III)
(2) Small dashed line corresponds to case without two temperature i.e. when $a_1 = 0 = a_3$.
(3) Solid line with centre symbol circle corresponds to the case of without energy dissipation (GN II)

Phase velocity

Figs. 2-4 indicate the variations of phase velocities V_1, V_2, V_3 with respect to frequency ω respectively. From Fig. 2, we notice that the variations of phase velocity V_1 decrease for the range $1 \leq \omega \leq 4$ and increase monotonically in the rest. We also notice that the values of phase velocity V_1 corresponding to GN II are maximum whereas are minimum corresponding to GN III for the whole range. Variations are similar corresponding to GN II and GN III whereas are somewhat different in absence of two temperature parameter. Fig. 3, exhibits the variations of phase velocity V_2 with respect to frequency ω. Here, we notice that variations steadily decrease and approach boundary surface with increase in wave number. Fig. 4, shows variations of phase velocity V_3 with respect to frequency ω. Here we notice that the values of phase velocity are increasing monotonically with similar trends corresponding to all the cases with change in magnitude. Phase velocity V_3 attains maximum values corresponding to GN III and attains minimum values corresponding to GN II whereas the values corresponding to $a_1 = 0 = a_3$ lie in between these two.

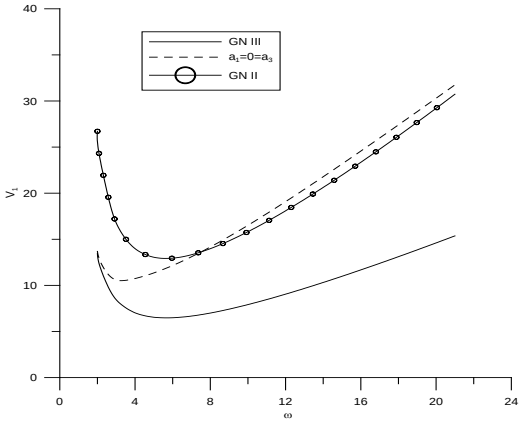

Fig. 2 Variations of phase velocity V_1 with respect to frequency ω

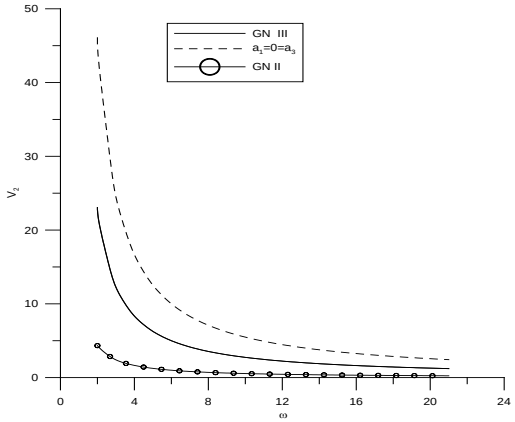

Fig. 3 Variations of phase velocity V_2 with respect to frequency ω

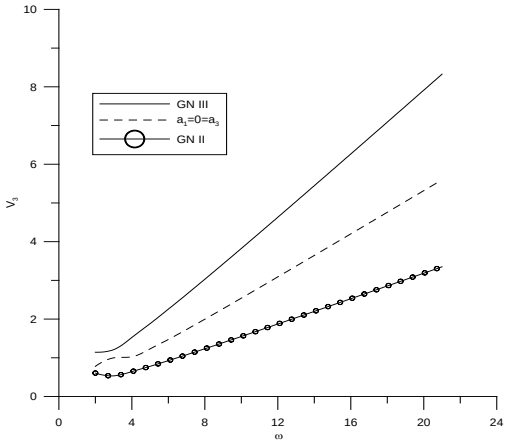

Fig. 4 Variations of phase velocity V_3 with respect to frequency ω

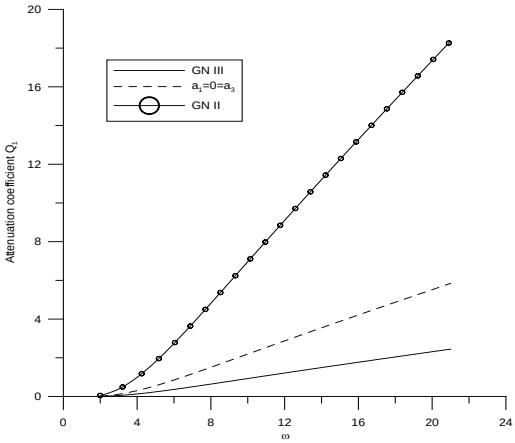

Fig. 5 Variations of attenuation coefficient Q_1 with respect to frequency ω

Attenuation coefficients

Fig. 5 shows that the values of attenuation coefficient Q_1 increase monotonically with respect to frequency ω. Maximum values are obtained corresponding to GN II and minimum are obtained for GN III. Trends of variations are noticed similar while investigating all the cases. Fig. 6 exhibits the trends of attenuation coefficient Q_2 with respect to frequency ω. Initially, the difference in values corresponding to all the cases is negligible but a significant difference is noticed with increase of wave number. Corresponding to GN II and GN III, initially, there is an increase for the range $2 \leq \omega \leq 3$, followed by a decrease for the range $3 \leq \omega \leq 4$ and increase in the rest. Corresponding to GN II, variations are noticed maximum. For, absence of two temperature, the values of Q_2 increase monotonically. Fig. 7 represents the variations of attenuation coefficient Q_3 with respect to frequency ω. Here, corresponding to all the cases, variations increase monotonically with maximum variations corresponding to GN II and minimum corresponding to absence of two temperature.

Specific loss

Fig. 8 exhibits the variations of Specific loss R_1 with respect to frequency ω. Here, we notice that the variations increase monotonically corresponding to all the cases. Fig. 9 shows Variations of Specific loss R_2 with respect to frequency ω. Here the trends are similar to Fig8 corresponding to GN II and absence of two temperature whereas corresponding to GN III, we notice that a decrease for the range $1 \leq \omega \leq 2$ is followed by an increase for the range $2 \leq \omega \leq 4$, and after achieving maximum value at $\omega = 4$, a smooth decrease follows approaching boundary surface. Fig. 10 shows Variations of Specific loss R_3 with respect to frequency ω. Here, we notice that, variations increase smoothly corresponding to the case GN III whereas opposite trends are noticed corresponding to $a_1 = 0 = a_3$ and GN II.

Penetration depth

Fig. 11 shows the variations of penetration depth S_1 with respect to frequency ω. Here,we notice that there is a sharp decrease in the values of S_1 corresponding to all the cases for the range

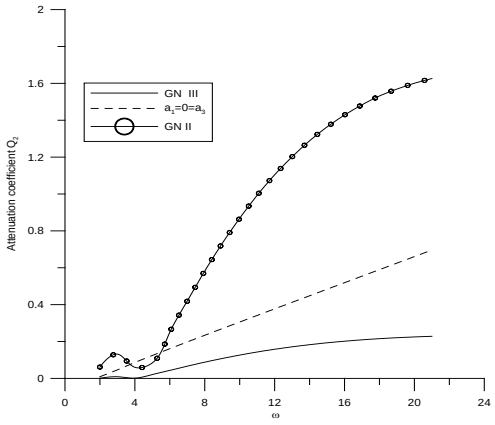

Fig. 6 Variations of attenuation coefficient Q_2 with respect to frequency ω

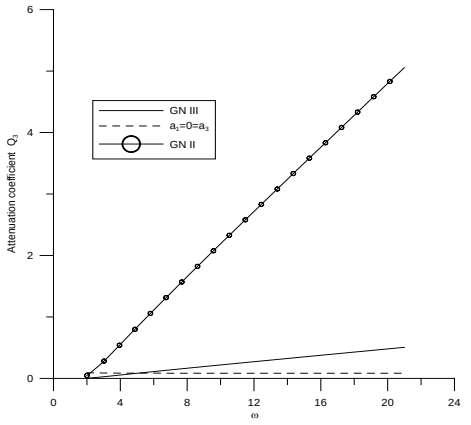

Fig. 7 Variations of attenuation coefficient Q_3 with respect to frequency ω

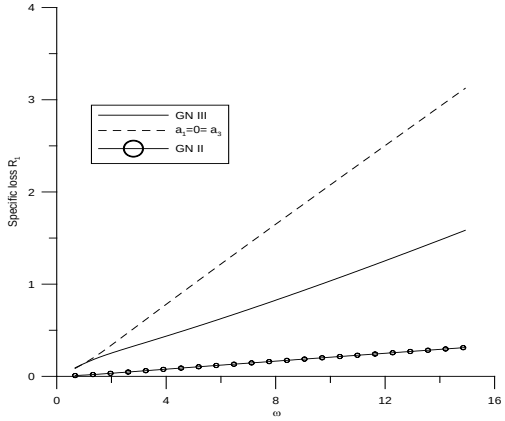

Fig. 8 Variations of specific loss R_1 with respect to frequency ω

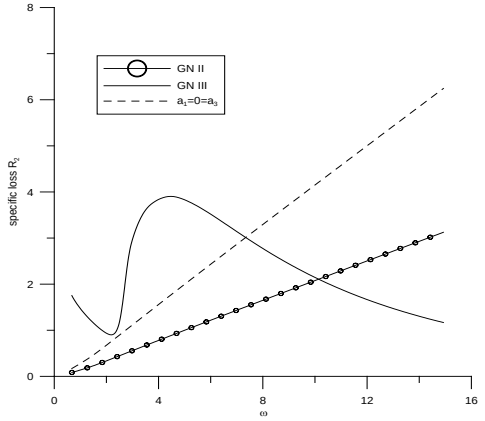

Fig. 9 Variations of specific loss R_2 with respect to frequency ω

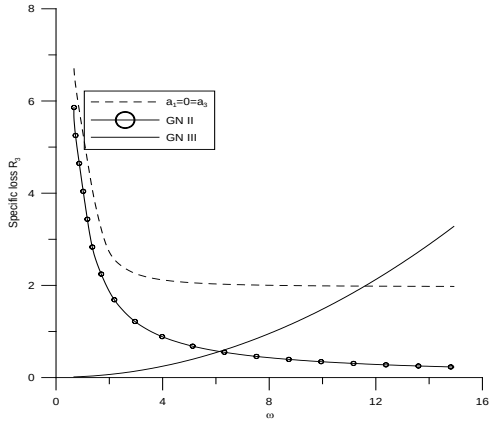

Fig. 10 Variations of specific loss R_3 with respect to frequency ω

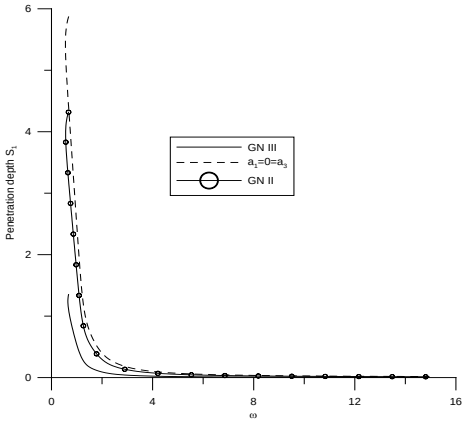

Fig. 11 Variations of penetration depth S_1 with respect to frequency ω

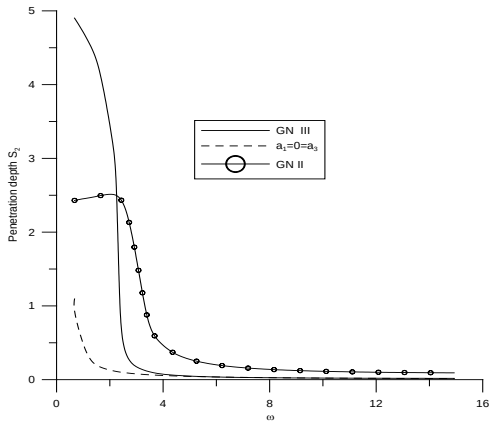

Fig. 12 Variations of penetration depth S_2 with respect to frequency ω

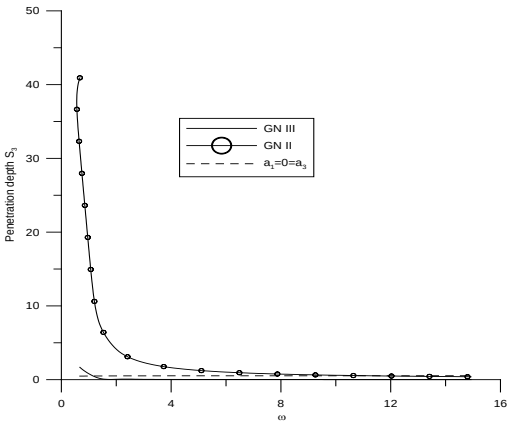

Fig. 13 Variations of penetration depth S_3 with respect to frequency ω

$1 \leq \omega \leq 3$, and the variations approach the boundary surface by decreasing slowly and smoothly in the rest. Fig. 12 shows the variations of penetration depth S_2 with respect to frequency ω. We notice that, initially, the values are constant and there is a sharp decrease afterwards which is followed by smooth decrease approaching the boundary surface in all the cases. Fig. 13 shows the variations of penetration depth S_3 with respect to ω.Here the variations are similar as discussed in Fig. 11.

Energy ratios

Incident QL wave

Fig. 14 depicts the Variations of Energy ratio E_{11} with respect to angle of incidence θ. It shows that the values of E_{11} increase slowly and smoothly corresponding to the cases of GN II and absence of two temperature whereas trends are opposite corresponding GN III. Also maximum values are noticed in case of absence of two temperature. Fig. 15 shows the variations of energy ratio E_{12} with respect to angle of incidence θ. Here the variations are similar as discussed in Fig.

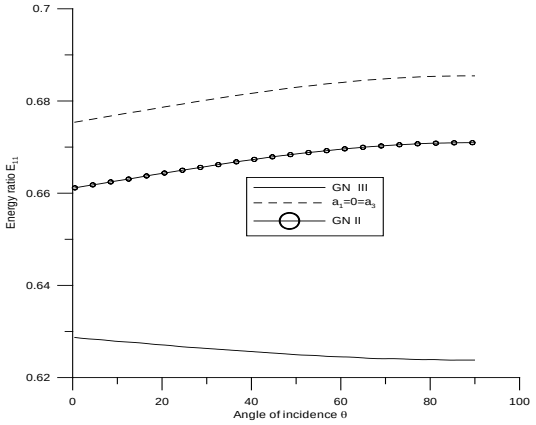

Fig. 14 Variations of energy ratio E_{11} with respect to angle of incidence θ

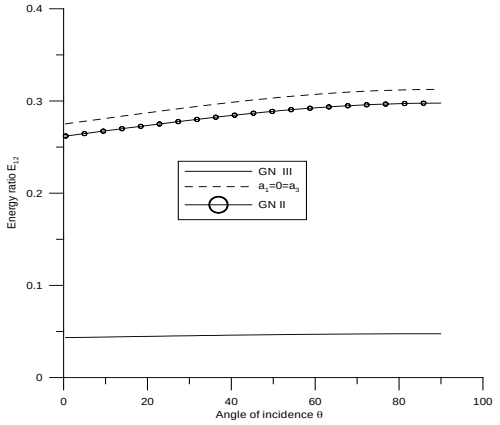

Fig. 15 Variations of energy ratio E_{12} with respect to angle of incidence θ

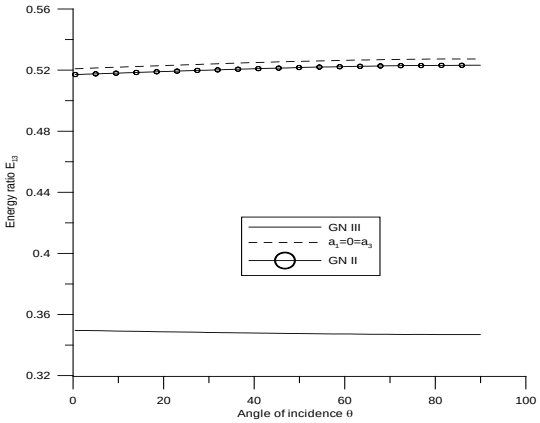

Fig. 16 Variations of energy ratio E_{13} with respect to angle of incidence θ

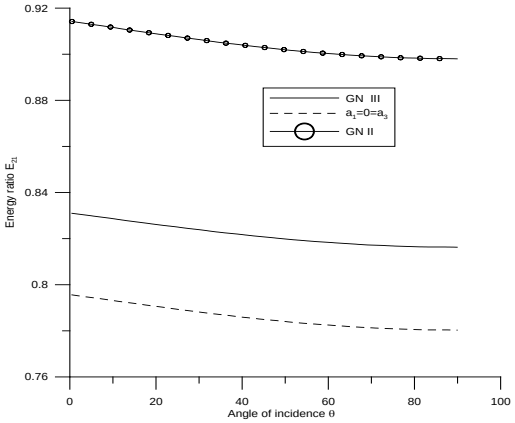

Fig. 17 Variations of energy ratio E_{21} with respect to angle of incidence θ

14. Fig. 16 depicts the Variations of Energy ratio E_{13} with respect to angle of incidence θ. It is noticed that the values of E_{13} have minimum variations nearly remain constant throughout the range.

Incident QTS wave

Fig. 17 depicts the Variations of Energy ratio E_{21} with respect to angle of incidence θ. Here corresponding to all the cases, we notice similar slowly decreasing trends with difference in magnitudes for the whole range. Fig. 18 depicts the Variations in Energy ratio E_{22} with respect to angle of incidence θ. Here corresponding to all the cases, trends are opposite as discussed in Fig. 17. Variations of Energy ratio E_{23} with respect to angle of incidence $\theta$are shown in Fig. 19. Here, we notice small variations corresponding to all the cases.

Incident QT wave

Figs. 20-22 depict the Variations of Energy ratios E_{31}, E_{32}, E_{33} with respect to angle of

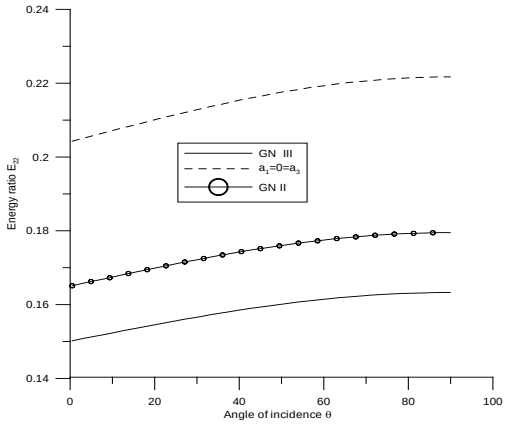

Fig. 18 Variations of energy ratio E_{22} with respect to angle of incidence θ

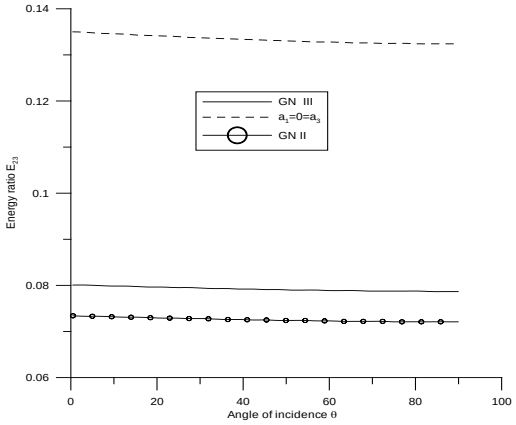

Fig. 19 Variations of energy ratio E_{23} with respect to angle of incidence θ

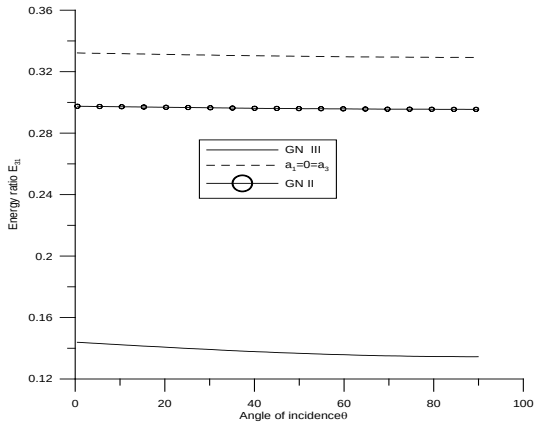

Fig. 20 Variations of Energy ratio E_{31} with respect to angle of incidence θ

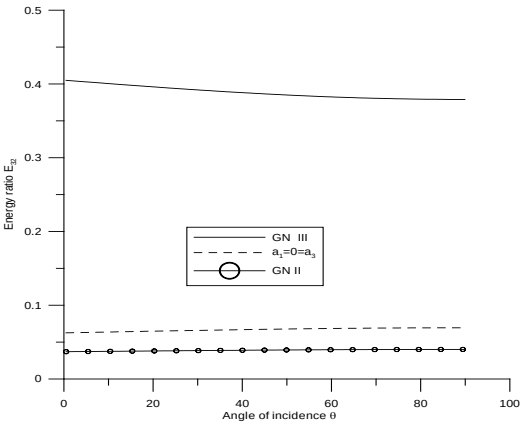

Fig. 21 Variations of Energy ratio E_{32} with respect to angle of incidence θ

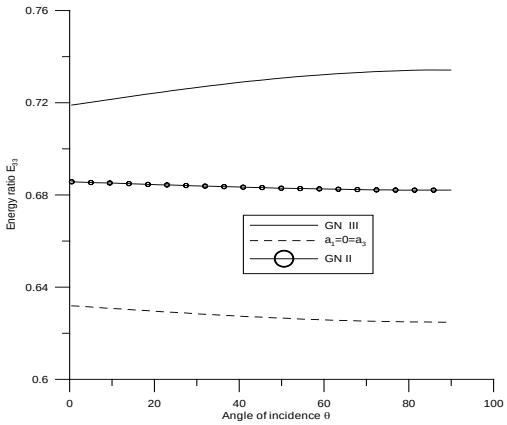

Fig. 22 Variations of energy ratio E_{33} with respect to angle of incidence θ

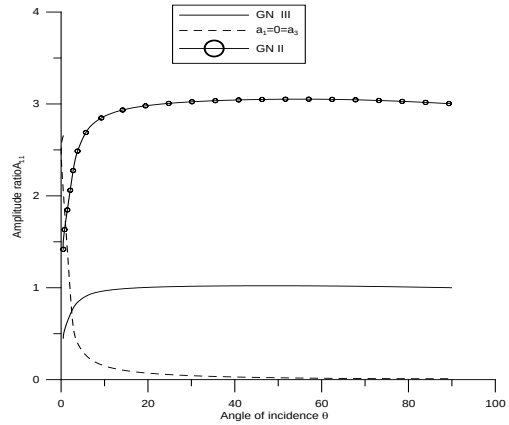

Fig. 23 Variations of amplitude ratio A_{11} with respect to angle of incidence

incidence θ. Here, in all the figures, similar trends of small variations are noticed with change in magnitude corresponding to different cases.

Amplitude ratios

Incident QL wave

Fig. 23 shows variations of amplitude ratio A_{11} with respect to angle of incidence θ. Here, we notice that, initially, there is a sharp increase in the values of A_{11} for the range $0^0 \leq \theta \leq 10^0$ corresponding to the cases of GN II and GN III, and afterwards the values have only small variations. Opposite trends are noticed for the case of absence of two temperature. Fig. 24 depicts variations of amplitude ratio A_{12} with respect to angle of incidence θ. Here, we notice that, the values of amplitude ratio increase monotonically for the range $0^0 \leq \theta \leq 40^0$ and after achieving maximum value at 40^0, the values start decreasing and approach boundary surface. Variations of amplitude ratio A_{13} with respect to angle of incidence θ are shown in Fig. 25. Here, we notice

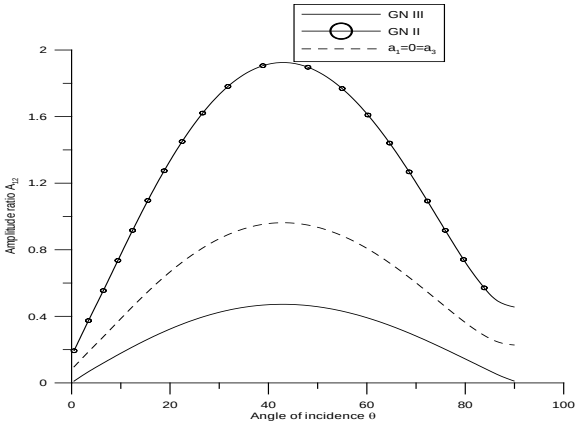

Fig. 24 Variations of amplitude ratio A_{12} with respect to angle of incidence

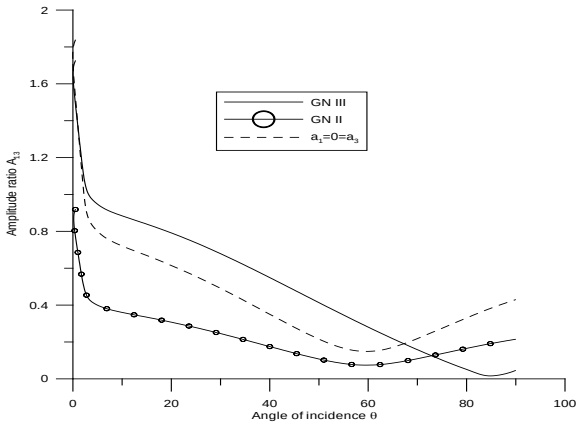

Fig. 25 Variations of amplitude ratio A_{13} with respect to angle of incidence

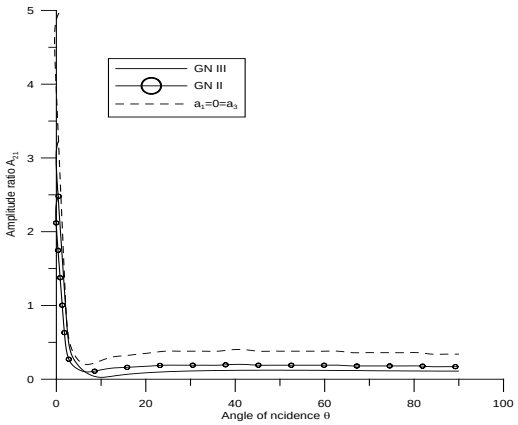

Fig. 26 Variations of amplitude ratio A_{21} with respect to angle of incidence

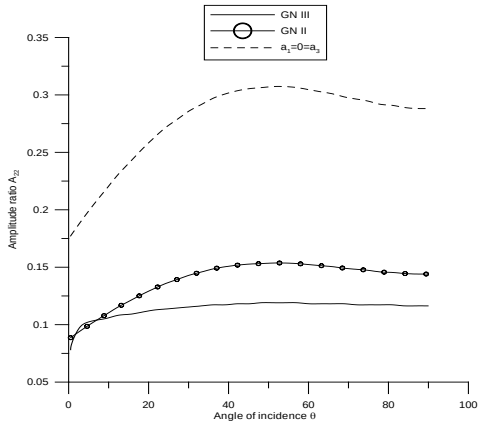

Fig. 27 Variations of amplitude ratio A_{22} with respect to angle of incidence

that a sharp decrease in the beginning is followed by a linear decrease and in the last phase, the values increase monotonically corresponding to all the cases GN II, GN III, and $a_1 = 0 = a_3$.

Incident QTS wave

Fig. 26 depicts the variations of amplitude ratio A_{21} with respect to angle of incidence θ. Here, we notice that a sharp decrease in the values of amplitude ratios in the beginning is followed by a slow and small increasing variations. We notice these trends while investigating the effect of GN II, GN III, and $a_1 = 0 = a_3$. Fig. 27 shows the variations of amplitude ratio A_{22} with respect to angle of incidence θ. Here, we notice that a smooth increase in the variations of amplitude ratio is followed by a smooth decrease corresponding to the cases GN II and $a_1 = 0 = a_3$ whereas, we notice small variations corresponding to the case of GN III. Fig. 28 shows the variations in amplitude ratio A_{23} with respect to angle of incidence θ. The variations in this figure are similar as discussed in Fig. 26 with change in magnitude.

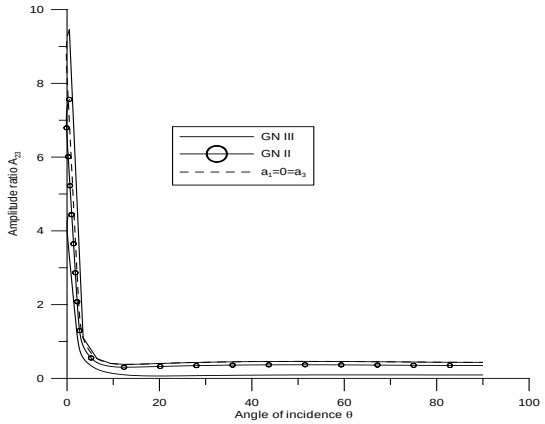

Fig. 28 Variations of amplitude ratio A_{23} with respect to angle of incidence

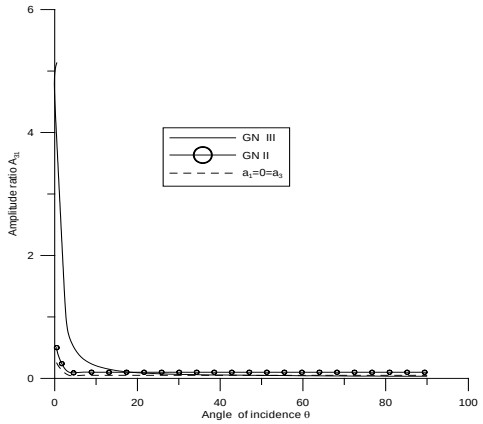

Fig. 29 Variations of amplitude ratio A_{31} with respect to angle of incidence

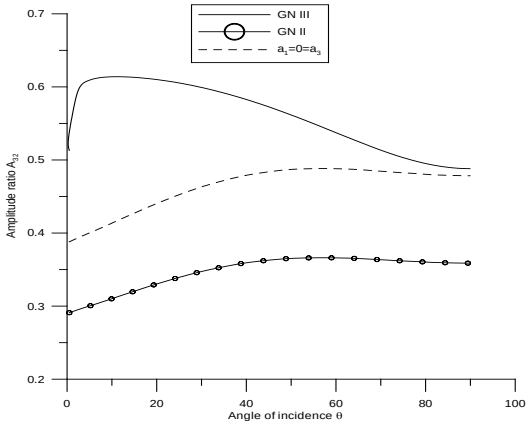

Fig. 30 Variations of amplitude ratio A_{32} with respect to angle of incidence

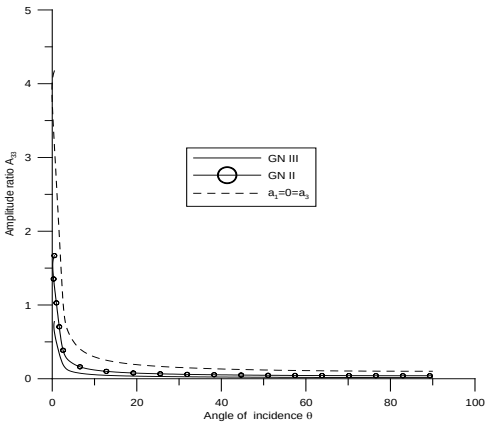

Fig. 31 Variations of amplitude ratio A_{33} with respect to angle of incidence

Incident QT wave

Fig. 29-31 show the variations of amplitude ratios A_{31}, A_{32} and A_{33} with respect to angle of incidence θ respectively. Here, the variations in Figs. 29 and 31 are similar as discussed in Fig. 26 whereas Fig. 30 shows different trends. Here, we notice that corresponding to GN II and $a_1 = 0 = a_3$, the trends are smoothly increasing whereas corresponding to GN III, we notice that sharp increase in the beginning is followed by a smooth decrease.

8. Conclusions

From the graphs, we observe that while investigating the surface of earth having different layers (anisotropy) and interfaces, elastic waves propagating through the earth have different velocities and are influenced by the properties of the layer through which they travel. Frequency of waves produced in the material have significant impact on the phase velocity, attenuation coefficients, specific loss and penetration depth of various kinds of waves. Also the magnitude of energy ratios is in the impact of angle of incidence. As angle of incidence increases, we notice less variation in the magnitudes of energy ratios. Two temperature parameter changes the magnitude of waves. The signals of these waves are not only helpful in providing information about the internal structures of the earth but also helpful in exploration of valuable materials such as minerals, crystals and metals etc.

References

Achenbach, J.D. (1973), *Wave Propagation in Elastic Solids*, Elsevier, North-Holland, Amsterdam, The Netherlands.

Atwa, S.Y. and Jahangir, A. (2014), "Two temperature effects on plane waves in generalized thermo-microstretch elastic solid", *Int. J. Thermophys.*, **35**(1), 175-193.

Boley, B.A. and Tolins, I.S. (1962), "Transient coupled thermoelastic boundary value problem in the half space", *J. Appl. Mech.*, **29**(4), 637-646.

Chandrasekharaiah, D.S. (1998), "Hyperbolic thermoelasticity: A review of recent literature", *Appl. Mech. Rev.*, **51**(12), 705-729.

Chen, P.J. and Gurtin, M.E. (1968), "On a theory of heat conduction involving two parameters", *Zeitschrift für angewandte Mathematik und Physik* (*ZAMP*), **19**, 614-627.

Chen, P.J., Gurtin, M.E. and Williams, W.O. (1968), "A note on simple heat conduction", *J. Appl. Math. Phys.* (*ZAMP*), **19**(6), 969-970.

Chen, P.J., Gurtin, M.E. and Williams, W.O. (1969), "On the thermodynamics of non simple elastic materials with two temperatures", *J. Appl. Math. Phys.* (*ZAMP*), **20**(1), 107-112.

Das, P. and Kanoria, M. (2014), "Study of finite thermal waves in a magnetothermoelastic rotating medium", *J. Therm. Stress.*, **37**(4), 405-428.

Dhaliwal, R.S. and Singh, A. (1980), *Dynamic Coupled Thermoelasticity*, Hindustance Publisher Corp., New Delhi, India, 726 p.

Green, A.E. and Naghdi, P.M. (1991), "A re-examination of the basic postulates of thermomechanics", *Proceedings of Royal Soc. A - London Ser.*, **432**(1885), pp. 171-194.

Green, A.E. and Naghdi, P.M. (1992), "On undamped heat waves in an elastic solid", *J. Therm. Stress.*, **15**(2), 253-264.

Green, A.E. and Naghdi, P.M. (1993), "Thermoelasticity without energy dissipation", *J. Elast.*, **31**(3), 189-208.

Kaushal, S., Sharma, N. and Kumar, R. (2010), "Propagation of waves in generalized thermoelastic continua

with two temperature", *Int. J. Appl. Mech. Eng.*, **15**(4), 1111-1127.
Kaushal, S., Kumar, R. and Miglani, A. (2011), "Wave propagation in temperature rate dependent thermoelasticity with two temperatures", *Math. Sci.*, **5**(2), 125-146.
Keith, C.M. and Crampin, S. (1977), "Seismic body waves in anisotropic media, reflection and refraction at a plane interface", *Geophys. J. R. Astr. Soc.*, **49**(1), 181-208.
Kumar, R. (2015), "Wave propagation in a microstretch thermoelastic diffusion solid", *VERSITA*, **23**(1), 127-169.
Kumar, R. and Gupta, V. (2013), "Plane wave propagation in an anisotropic thermoelastic medium with fractional order derivative and void", *J. Thermoelast.*, **1**(1), 21-34.
Kumar, R. and Kansal, T. (2011), "Reflection of plane waves at the free surface of a transversely isotropic thermoelastic diffusive solid half-space", *Int. J. Appl. Math. Mech.*, **7**(14), 57-78.
Kumar, R. and Mukhopdhyay, S. (2010), "Effects of thermal relaxation times on plane wave propagation under two temperature thermoelasticity", *Int. J. Eng. Sci.*, **48**(2), 128-139.
Kumar, R., Sharma, N. and Ram, P. (2008), "Reflection and transmission of micropolar elastic waves at an imperfect boundary", *Multidiscipl. Model. Mater. Struct.*, **4**(1), 15-36.
Lee, J. and Lee, S. (2010), "General solution of EM wave propagation in anisotropic media", *J. Kor. Phys. Soc.*, **57**(1), 55-60.
Marin, M. (1995), "On existence and uniqueness in thermoelasticity of micropolar bodies", *Comptes Rendus, Acad. Sci. Paris, Serie II*, **321**(12), 475-480.
Marin, M. (1996), "Some basic theorems in elastostatics of micropolar materials with voids", *J. Comp. Appl. Math.*, **70**(1), 115-126.
Marin, M. (2010), "Lagrange identity method for microstretch thermoelastic materials", *J. Math. Anal. Appl.*, **363**(1), 275-286.
Marin, M. and Marinescu, C. (1998), "Thermoelasticity of initially stressed bodies. Asymptotic equipartition of energies", *Int. J. Eng. Sci.*, **36**(1), 73-86.
Othman, M.I.A. (2010), "Generalized Electro-Magneto-Thermoelasticity in case of thermal shock wavesfor a finite conducting half-space with two relaxation times", *Mech. Mech. Eng.*, **14**(1), 5-30.
Sharma, K. and Bhargava, R.R. (2014), "Propagation of thermoelastic plane waves at an imperfect boundary of thermal conducting viscous liquid/generalized thermolastic solid", *Afrika Mathematika*, **25**(1), 81-102.
Sharma, K. and Kumar, P. (2013), "Propagation of plane waves and fundamental solution in thermoviscoelastic medium with voids", *J. Therm. Stress.*, **36**(2), 94-111.
Sharma, K. and Marin, M. (2013), "Effect of distinct conductive and thermodynamic temperatures on the reflection of plane waves in micropolar elastic half-space", *U.P.B. Sci. Bull Series*, **75**(2), 121-132.
Sharma, S., Sharma, K. and Bhargava, R.R. (2013), "Effect of viscousity on wave propagation in anisotropic thermoelastic with Green-Naghdi theory type-II and type-III", *Mater. Phys. Mech.*, **16**(2), 144-158.
Singh, S.S. and Krosspanie, L. (2013), "Phase velocity of harmonic waves in monoclinic anisotropic medium", *Sci. Vis.*, **13**(3), 133-136.
Slaughter, W.S. (2002), *The Linearised Theory of Elasticity*, Birkhausar.
Warren, W.E. and Chen, P.J. (1973), "Wave propagation in the two temperature theory of thermoelasticity", *J. Acta Mech.*, **16**(1), 21-33.
Youssef, H.M. (2006), "Theory of two temperature generalized thermoelasticity", *IMA J. Appl. Math.*, **71**(3), 383-390.
Youssef, H.M. (2011), "Theory of two - temperature thermoelasticity without energy dissipation", *J. Therm. Stress.*, **34**(2), 138-146.
Zakaria, M. (2014), "Effect of hall current on generalized magneto thermoelastic micropolar solid subjected to ramp type heating", *Int. Appl. Mech.*, **50**(1), 92-104.

CC